



Penetrating Microindentation of Hyper-soft, Conductive Silicone Neural Interfaces *in Vivo* Reveals Significantly Lower Mechanical Stresses

Arati Sridharan¹, Vikram Kodibagkar², Jit Muthuswamy¹

¹*Neural Microsystems Laboratory, School of Biological & Health Systems Engineering, 501 E Tyler Mall, Arizona State University, Tempe, AZ, USA, 85287*

²*Prognostic BioEngineering (ProBE) laboratory, School of Biological & Health Systems Engineering, 501 E Tyler Mall, Arizona State University, Tempe, AZ, USA, 85287*

ABSTRACT

There is growing evidence that minimizing the mechanical mismatch between neural implants and brain tissue mitigates inflammatory, biological responses at the interface under long-term implant conditions. The goal of this study is to develop a brain-like soft, conductive neural interface and use an improvised, penetrating microindentation technique reported by us earlier to quantitatively assess the (a) elastic modulus of the neural interface after implantation, (b) mechanical stresses during penetration of the probe, and (c) periodic stresses at steady-state due to tissue micromotion around the probe. We fabricated poly-dimethylsiloxane (PDMS) matrices with multi-walled carbon nanotubes (MWCNTs) using two distinct but carefully calibrated cross-linking ratios, resulting in hard (elastic modulus~484 kPa) or soft, brain-like (elastic modulus~5.7 kPa) matrices, the latter being at least 2 orders of magnitude softer than soft neural interfaces reported so far. Subsequent loading of the hard and soft silicone based matrices with (100% w/w) low-molecular weight PDMS siloxanes resulted in further decrease in the elastic modulus of both matrices. Carbon probes with soft PDMS coating show significantly less maximum axial forces ($-587 \pm 51.5 \mu\text{N}$) imposed on the brain than hard PDMS coated probes ($-1,253 \pm 252 \mu\text{N}$) during and after insertion. Steady-state, physiological micromotion related stresses were also significantly less for soft-PDMS coated probes ($55.5 \pm 17.4 \text{ Pa}$) compared to hard-PDMS coated probes ($141.0 \pm 21.7 \text{ Pa}$). The penetrating microindentation technique is valuable to quantitatively assess the mechanical properties of neural interfaces in both acute and chronic conditions.

INTRODUCTION

Mitigation of failure modes at the implant interface is a key challenge for the biomedical industry, emphasizing the need to develop biocompatible, implantable interfaces. Inflammation near neural interfaces is hypothesized to result in deterioration of electrical performance of neural implants used for recording or stimulating neurons. Several studies have shown implanted microelectrode arrays have unstable impedances under chronic conditions and loss of neural activity [1,2]. Our previous study showed that the elastic modulus of the neural interface dynamically changes with time [3]. Multiple, different engineering solutions have been proposed such as making the electrode small, using ‘stealth’ strategies with acellular or hydrogel (i.e. matrigel) or polydimethylsiloxane (e-dura) scaffolds, making the electrode material tunably soft ranging from 20 MPa to 974 kPa [4–8] or coating the electrode with a soft PEG based material or ‘fuzzy’ polymers [9,10]. However, a recent study has suggested a limit to the improvement in foreign body response observed in the brain tissue that can be achieved by decreasing the elastic modulus of the probe material [11]. In this study we compared carbon fibers coated with silicone-based (polydimethylsiloxane) matrices with carefully calibrated cross-linking strengths to achieve two different elastic moduli (~5.7 kPa and ~484 kPa) that were made conductive using multi-walled carbon nanotubes (MWCNTs). Using an improvised, penetrating microindentation technique we reported earlier [3,12], we subsequently assessed the mechanical stress response of brain tissue to the soft-PDMS ($E\sim 5.7$ kPa) coated implants and hard-PDMS coated implants ($E\sim 484$ kPa) with similar dimensions. The PDMS matrices offer an opportunity to load molecular sensors such as low-molecular weight siloxanes (LMW-siloxane) that are used as MRI contrast agents [13–15]. In this study, addition of the LMW-siloxanes to the silicone matrices further decreased the elastic moduli of the soft matrix to ~1.6 kPa and of the hard matrix to ~331 kPa. Carbon fiber probes that were coated with soft, silicone matrices imposed significantly less forces at the brain-tissue interface based on microindentation *in vivo*.

EXPERIMENTAL DETAILS

Silicone Coating Preparation

Soft and hard silicone matrices were fabricated from PDMS precursors (Sylgard™ 184 elastomer kit, Dow Corning) using the crosslinker to base ratios of 1:10 (w/w) and 1:75 (w/w). Multi-walled carbon nanotubes (MWCNTs) (CheapTubes.com, Grafton, VT) were treated with nitric and sulfuric acid to functionalize the MWCNTs with a carboxylic acid group. The functionalized nanotubes were incorporated at <1 mg/g of pre-mixed PDMS precursors prior to curing. For determining elastic modulus, samples were poured into circular disk molds (~5 cm diameter, 1 cm thickness) and cured overnight. LMW-siloxane (410 g/mol, Cas no. 9016-00-6) was loaded at 100% (w/w) into some samples of cured PDMS matrices. For animal experiments, 7 μ m thick carbon fibers were epoxied together to form bundles with ellipsoidal cross-sections having major and minor axes of $\sim 100 \times 10$ μ m respectively. The bundled fibers were coated with either hard PDMS (1:10 crosslinker-to-base ratio with MWCNTs) or soft PDMS (1:75 crosslinker-to-base ratio with MWCNTs) material to form a final probe with an ellipsoidal cross-section having major and minor axes of $\sim 500 \times 120$ μ m respectively. Some of the coated fiber-bundles were loaded at 100% (w/w) with LMW-siloxane and representative images are shown in figure 2 inset.

Mechanical Characterization

To quantitatively assess the mechanical properties of the silicone materials, conventional microindentation technique was performed using a 3 mm diameter spherical, stainless steel indenter (inset of figure 1) at a constant rate of 10 $\mu\text{m/sec}$. The samples were indented 200 μm and force-displacement curves were obtained using a Futek™-10 g load cell (Futek LSB210, Irvine, CA). A total of 5 force-displacement curves were obtained for samples from each of 4 categories (hard PDMS matrices with/without LMW-siloxane and soft PDMS matrices with/without LMW-siloxane). To calculate elastic modulus, the Hertzian spherical indentation model was used

$$\frac{P}{\pi a^2} = \frac{4}{3} \pi E \left(\frac{a}{r} \right) \quad (1)$$

where P is force, a is contact radius, E is the composite modulus (of silicone-MWCNT), and r is the radius of the indenter at 200 μm depth [16]. Poisson's ratio of the brain tissue was assumed to be 0.5.

All animal experiments were performed with the approval of the Institute of Animal Care and Use Committee of Arizona State University (IACUC). A C57Bl6 strain male mouse (\sim 43g) was injected intraperitoneally with a cocktail containing 42 mg/kg ketamine, 4.8 mg/kg xylazine, 0.6 mg/kg acepromazine to induce anesthesia and was subsequently maintained using isoflurane (0.5 L/min). After immobilizing in a stereotaxic frame, skin and soft tissue is removed to expose the skull. A large craniotomy between bregma and lambda suture lines on either hemisphere was performed. The edges of the craniotomy were \sim 1 mm from the bregma, lambda, midline sutures. To characterize the mechanical properties of the neural interface *in vivo*, an improvised, penetrating microindentation technique was used [3,12]. A total of 8 force-displacement curves were recorded from 8 regions spaced at least 1 mm apart and 2.5 lateral to midline in both hemispheres. Relative locations for hard and soft PDMS probes on the mouse skull are sketched in inset of figure 2. Force-displacement curves ($n=4$) for either hard PDMS coated or soft PDMS coated carbon fibers loaded with LMW-siloxane were obtained during the insertion of the probe (speed of 10 $\mu\text{m/sec}$) into the cortex of a mouse brain for a depth of 1 mm. One force-displacement curve from a soft-coated probe was discarded due to delamination of the coating. After the movement was stopped, viscoelastic relaxation forces along with breathing and heart-rate induced micromotion forces were recorded and analysed. Elastic modulus of the brain tissue, E_{brain} was estimated from the first 200 μm of the force-displacement curve corresponding to the indentation phase (indentation or dimpling of the brain tissue just preceding penetration [3]). Assuming small deformations, for any axisymmetric indenter the effective elastic modulus (E_{brain}) is related to the contact area (A) and stiffness defined as the change in force (P) relative to indentation depth (H) (derived from force curves) [16] :

$$E_{\text{brain}} = \frac{\sqrt{\pi}}{2\beta} \frac{(dP/dH)}{\sqrt{A}} \quad (2)$$

The contact area is estimated from the geometric surface area of a cylinder with 500 μm \times 120 μm ellipsoidal cross-section at different indentation depths. β is a correction factor, which is typically taken to be unity for ideal indenters. Elastic moduli, E^* are also estimated from the instantaneous shear modulus (G_0) in the force-displacement curves measured at 1 mm insertion depth immediately after the termination of movement for

both hard- and soft-coated carbon fibers. Assuming a linear viscoelastic system and $\nu_{brain} \sim 0.5$,

$$E^* \sim 2(1 + \nu)G_0 \quad (3)$$

In principle, the elastic modulus estimated using the above method is the effective elastic modulus, E^* due to the combined effect of the material properties of both the indenter (probe) and the brain tissue as defined by [16]:

$$\frac{1}{E^*} = \frac{1 - \nu_{brain}^2}{E_{brain}} + \frac{1 - \nu_{indenter}^2}{E_{indenter}} \quad (4)$$

where ν_{brain} is 0.5 assuming incompressibility of brain tissue and $\nu_{indenter}$ is varied between 0.2 - 0.45 to account for the composite properties of carbon fiber and silicone coatings. As elastic modulus of the indenter, $E_{indenter}$ increases the effective elastic modulus, E^* is expected to approach the elastic modulus of the brain (E_{brain}) as illustrated in figure 3.

RESULTS

The elastic moduli of (a) hard PDMS matrices with a (1:10) crosslinker-to-base ratio mixed with functionalized MWCNTs and (b) soft PDMS matrices with a (1:75) crosslinker-to-base ratio mixed with functionalized MWCNTs with and without loading of LMW-siloxane are shown in figure 1. The median elastic modulus of 5 samples of hard PDMS was 454 kPa compared to 5.7 kPa for soft PDMS matrices. The addition of LMW-siloxane (100% w/w loading) to both matrices significantly reduced the elastic moduli to 331 kPa (hard PDMS) and 1.6 kPa (soft PDMS). Marginal swelling of the matrices (~1-3% geometric swelling) was observed at 100% loading.

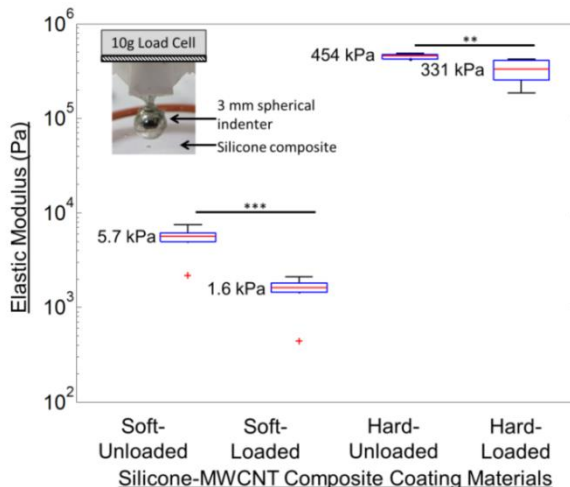


Figure 1. Box plots of elastic moduli for soft and hard silicone-MWCNT matrix composites loaded with and without low molecular weight (LMW) siloxanes (1:1 w/w) ($n=5$ samples each category). LMW siloxane loaded silicone-MWCNT composite matrices were significantly softer than unloaded matrices for both hard

(** $p<0.01$) and soft (** $p<0.001$) composite matrices. Elastic moduli were calculated using the spherical microindentation technique (inset) and equation 1.

In the penetrating microindentation tests for assessing the mechanical properties of neural interfaces *in vivo*, the soft-PDMS and hard-PDMS coated fibers were inserted into the brain at different locations in the living mouse cortex at a constant speed of 10 $\mu\text{m/sec}$ (except one hard-coated sample at 15 $\mu\text{m/sec}$) till they reached a depth of 1 mm in the brain tissue, after which viscoelastic relaxation forces were recorded for 5 min (figure 2). Comparison of pre- and post-insertion images demonstrated that the mechanical integrity of the coating loaded with LMW-siloxanes is maintained during the insertion process, except one soft-PDMS coated probe which delaminated and was not included in further analysis. Soft-PDMS coated fibers showed significantly lower maximum forces ($-587 \pm 51.5 \mu\text{N}$) compared to hard-PDMS coated fibers ($-1,253 \pm 252 \mu\text{N}$) of similar dimensions both loaded with low molecular weight siloxanes. A close-up of the force-displacement curves at steady-state after termination of insertion, revealed periodic forces induced by breathing and heart-rate related tissue micromotion. The amplitudes of these forces were significantly less for soft-PDMS coated fibers ($61.9 \pm 19.5 \mu\text{N}$) compared to hard-PDMS coated fibers ($157.2 \pm 24.2 \mu\text{N}$) ($p<0.01$), suggesting that the soft elastomer coatings enabled the interface to be more compliant dampening chronic, periodic, micromotion induced stressors around the implant. Table I compared relative micromotion related stress amplitudes of various probes including the hard- and soft- PDMS based coatings in this study. Despite the larger dimensions of the probes used in this study, the micromotion induced stresses for soft-PDMS coated probes were comparable to soft nanocomposites coatings that have been demonstrated to be associated with significantly lower foreign body reaction in brain tissue [4,12].

Table I: Comparison of peak stresses due to periodic tissue micromotion.

Probe	Elastic Modulus	Peak Stress Amplitudes (Pa)
Silicon*	$\sim 200 \text{ GPa}$	221.5 ± 27.8
PVAc-coated Silicon*	49-78 GPa	82.2 ± 15.0
Stiff Nanocomposite*	5.2 GPa	99.1 ± 44.3
Soft Nanocomposite*	12 MPa	49.8 ± 13.4
Hard PDMS-CNT coating on carbon fiber	331 kPa	141.0 ± 21.7
Soft PDMS-CNT coating on carbon fiber	1.6 kPa	55.5 ± 17.4

*Sridharan et al (2015) [12]

The relaxation force curves (indicative of rate of viscoelastic stress relaxation in response to a step-like indentation on brain tissue) were fitted to a 2nd order Prony series model and the viscoelastic parameters were estimated [3,12] . The mean short-term relaxation time constant was $12.04 \pm 5.97 \text{ sec}$ for soft-PDMS coated carbon fiber compared to $31.91 \pm 17.9 \text{ sec}$ for hard-PDMS coated fibers. The retardation in the tissue stress relaxation rate could be due to significantly larger maximum forces on the brain tissue and increased crosslinking of the silicone coating. Other mechanical factors that may play a role are relative slip or adhesion between tissue and implant at the interface, surface tension, surface hydrophilicity, geometry, and flexibility. Further studies are needed to understand the role of material viscoelasticity and its impact on implant biocompatibility at the interface.

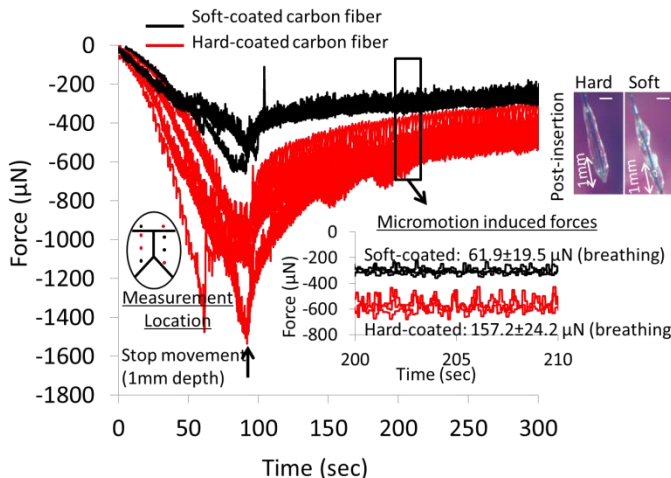


Figure 2. Measurement of forces as carbon-fiber probes (~100 $\mu\text{m} \times 20 \mu\text{m}$ width) coated with hard and soft silicone matrices loaded with low molecular weight siloxanes (~500 $\mu\text{m} \times 120 \mu\text{m}$ final dimensions) were advanced into the mouse brain *in vivo*. Data was collected at 4 locations (left inset) in the cortex in one animal. Data for one hard-coated probe (upper right inset) inserted at 15 $\mu\text{m/sec}$ was included in the analysis and is offset compared to other force curves. Upper right inset shows representative photographs of hard and soft-PDMS coated carbon probes post-insertion in the brain, reflecting mechanical integrity of coatings on probes. The coatings are ~5 times the thickness of the carbon fiber. Lower right inset shows close-up view of periodic forces induced by tissue micromotion corresponding to breathing for hard and soft PDMS coated probes (peak amplitudes of $157.2 \pm 24.2 \mu\text{N}$ and $61.9 \pm 19.5 \mu\text{N}$ respectively).

The effective elastic modulus (E^*) estimated from the shear modulus using equation 3 for soft-coated probes was lower ($1.6 \pm 0.179 \text{ kPa}$) compared to the E^* for hard-coated probes ($3.39 \pm 0.664 \text{ kPa}$) (figure 3). Since the elastic modulus of the soft-PDMS coated carbon probe (E_{indenter}) is comparable to that of the surrounding brain-tissue (E_{brain}), the measured axial forces (in figure 2) and the estimated effective elastic modulus, E^* (in figure 3) are lower (as explained by equation 4 and dotted line traces in figure 3). In contrast, the E^* corresponding to hard-PDMS coated probes is comparable to E_{brain} since E_{indenter} (for the hard-PDMS coated probes) in equation 4 is at least 2 orders of magnitude higher than E_{brain} . The effect of varying the Poisson's ratio for the indenter from 0.2 to 0.45 was not significant.

Interestingly, the mean elastic modulus of the brain tissue, E_{brain} estimated from the initial 200 μm indentation (just preceding insertion) in the force-displacement curves is $\sim 3.04 \text{ kPa}$ (figure 3, left inset) for both soft- and hard-coated probes, similar to the E^* derived for hard-PDMS coated probes. The above estimate of E_{brain} from the indentation phase of the force-displacement curve is expected to be dominated by bulk modulus effects (compressive pressure/ Δ volume) of the brain tissue compared to post-penetration phase of the probe, where the mechanical properties of the soft coating plays a more dominant role.

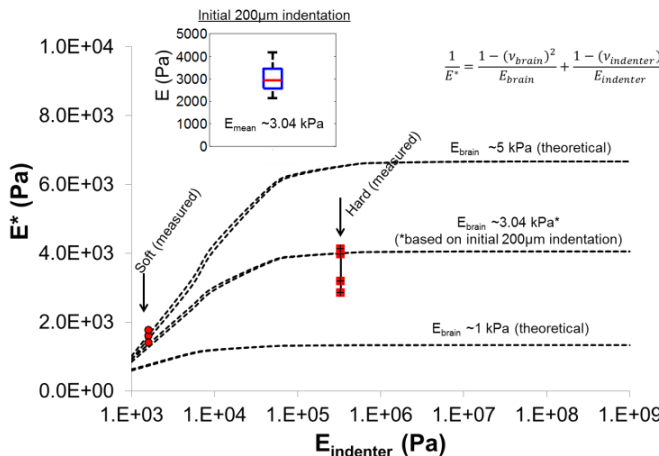


Figure 3. A plot of effective elastic modulus (E^*) as a function of elastic modulus of the indenter, E_{indenter} shows a reduction in E^* as the E_{indenter} approaches elastic modulus of brain tissue, E_{brain} . The red squares (hard coated probes, $n=4$) and red circles (soft-coated probes, $n=3$) show the effective elastic modulus (E^*) derived using equation 3 from the instantaneous shear modulus at 1 mm depth from force-displacement curves. E^* for soft-PDMS coated probes is $1600 \pm 179.6 \text{ Pa}$ while E^* for hard-PDMS coated probes is $3390 \pm 664.3 \text{ Pa}$. The dotted lines show effective elastic modulus (E^*) as a function of the E_{indenter} for $E_{\text{brain}} \sim 1-5 \text{ kPa}$ based on equation 4 (top right inset). The $E_{\text{brain}} = 3.04 \text{ kPa}$ is estimated using equation 2 from the initial indentation phase (first 200 μm of probe advancement) of the force-displacement curves corresponding to hard and soft coated probes. The upper left inset shows the boxplot distribution and mean for combined indentation based measurements from hard and soft probes ($n=7$). The mean E_{brain} from the indentation phase of force-displacement curves of soft coated probes was $3080 \pm 447 \text{ Pa}$ compared to $3000 \pm 1071 \text{ Pa}$ for hard coated probes.

CONCLUSIONS

The elastic moduli of PDMS-matrices incorporated with MWCNTs can be carefully modulated over a 100-fold range, to be brain-like in its viscoelastic properties by changing the crosslinker-to-base ratio from 0.1 to 0.013. Addition of LMW siloxanes marginally swells the matrix (~1-3% at 100% loading) decreasing the elastic component of its viscoelastic properties due to overstretch, leading to a Mullins-type softening effect of the cross-linked elastomer. Overall, soft-PDMS coated implants ($E \sim 1.6 \text{ kPa}$), which closely matches the elastic modulus of the brain-tissue, experience significantly lower axial mechanical forces and periodic micromotion induced stresses on brain tissue compared to other neural interface materials reported earlier.

ACKNOWLEDGEMENTS

Research was supported by NIH 1UF1NS107676-01 and NSF BRAIN I/UCRC 1650566.

References

- [1] K.A. Ludwig, J.D. Uram, J. Yang, D.C. Martin, and D.R. Kipke, *J. Neural Eng.* **3**, 59 (2006).
- [2] A. Prasad, Q.S. Xue, V. Sankar, T. Nishida, G. Shaw, W.J. Streit, and J.C. Sanchez, *J. Neural Eng.* **9**, 056015 (2012).
- [3] A. Sridharan, S.D. Rajan, and J. Muthuswamy, *J. Neural Eng.* **10**, 066001 (2013).
- [4] J.K. Nguyen, D.J. Park, J.L. Skousen, A.E. Hess-Dunning, D.J. Tyler, S.J. Rowan, C. Weder, and J.R. Capadona, *J. Neural Eng.* **11**, 056014 (2014).
- [5] Z.J. Du, C.L. Kolarcik, T.D.Y. Kozai, S.D. Luebben, S.A. Sapp, X.S. Zheng, J.A. Nabity, and X.T. Cui, *Acta Biomater.* **53**, 46 (2017).
- [6] A.J. Shoffstall, M. Ecker, V. Danda, A. Joshi-Imre, A. Stiller, M. Yu, J.E. Paiz, E. Mancuso, H.W. Bedell, W.E. Voit, J.J. Pancrazio, and J.R. Capadona, *Micromachines* **9**, 1 (2018).
- [7] S.A. Hara, B.J. Kim, J.T.W. Kuo, C.D. Lee, E. Meng, and V. Pikov, *J. Neural Eng.* **13**, 066020 (2016).
- [8] I.R. Minev, P. Musienko, A. Hirsch, Q. Barraud, N. Wenger, E.M. Moraud, J. Gandar, M. Capogrosso, T. Milekovic, L. Asboth, R.F. Torres, N. Vachicouras, Q. Liu, N. Pavlova, S. Duis, A. Larmagnac, J. Vörös, S. Micera, Z. Suo, G. Courtine, and S.P. Lacour, *Science* **347**, 159 (2015).
- [9] D. Kim, S. Richardson-Burns, L. Povlich, M. Abidian, S. Spanninga, J. Hendricks, and D. Martin, in *Indwelling Neural Implant. Strateg. Contend. with Vivo Environ*, edited by W. Reichert (CRC Press /Taylor& Francis, 2008),pp.177-220.
- [10] K.C. Spencer, J.C. Sy, K.B. Ramadi, A.M. Graybiel, R. Langer, and M.J. Cima, *Sci. Rep.* **7**, 12812 (2017).
- [11] H.C. Lee, F. Ejserholm, J. Gaire, S. Currin, J. Schouenborg, L. Wallman, M. Bengtsson, K. Park, J. Gaire, and K.J. Otto, *J. Neural Eng.* **14**, 36026 (2017).
- [12] A. Sridharan, J.K. Nguyen, J.R. Capadona, and J. Muthuswamy, *J. Neural Eng.* **12**, 036002 (2015).
- [13] V.D. Kodibagkar, W. Cui, M.E. Merritt, and R.P. Mason, *Magn. Reson. Med.* **55**, 743 (2006).
- [14] C.P. Addington, A. Cusick, R.V. Shankar, S. Agarwal, S.E. Stabenfeldt, and V.D. Kodibagkar, *Ann Biomed Eng.* **2016** **44**, 816 (2016).
- [15] V.D. Kodibagkar, X. Wang, J. s Pacheco-Torres, P. Gulaka, and R.P. Mason, *NMR Biomed.* **21**, 899 (2008).
- [16] W.C. Oliver and G.M. Pharr, *J. Mater. Res.* **19**, 3 (2004).